number. Instead the associative pathway of $k_{12}[L]$ (Scheme I) requires an increase in coordination number, which is presumably more readily achieved due to the large size of Re relative to the smaller Mn.[15]

Conclusion. Rather extensive kinetic studies were made of the reaction of (η^5-Ind)Re(CO)$_3$ with P(OEt)$_3$, and it was observed that at four different experimental conditions of temperature and P(OEt)$_3$ concentration the reaction progress and its products differ. Low temperatures and high concentrations of P(OEt)$_3$ favor the formation of η^1-**3**, whereas high temperatures and low concentrations of P(OEt)$_3$ favor the formation of η^5-**4**. The treatment of experimental data at four different reaction conditions allows for good agreement between experimental and simulated absorbancy changes during reaction, providing the η^1-**3** and η^5-**4** products come from the same active intermediate (Scheme I). The exact nature of this intermediate is not known, but on the basis of known ring-slippage[2] organometallic chemistry, it appears the intermediate should be η^3-**2**.

The nature of the entering nucleophile also plays a major role in the distribution of products η^1-**3** versus η^5-**4**. In general a nucleophile that is a strong base and has a small cone angle (P(CH$_3$)$_3$) favors formation of η^1-**3**, whereas one that is a weak base with a larger cone angle (P(OPh)$_3$) favors the η^5-**4** products. The kinetic indenyl ligand effect is observed to a lesser extent with trindenylmetal complexes, and in general the rates of reaction for analogous metal compounds decrease in the order Ind > Td > Cp. This is in accord with a decrease in π-delocalization of the electron density in the transition state/active intermediate for reaction. Finally, for the same system but different metal the rates of reaction decrease in the order Rh > Re > Mn. This order seems reasonable for these associative reactions with attack on the metal, because Rh is only 5-coordinate and because Re is larger than Mn.

Acknowledgment. We wish to thank Dr. Jeffrey W. Freeman for doing some of the preliminary kinetic experiments, Dr. Merritt C. Helvenston for preparing some of the compounds, and one of the reviewers for explaining the inductive contribution to the nucleophile specificity in the formation of η^1- or η^5-products. We also thank the National Science Foundation for its support of this research and Johnson-Matthey for the generous loan of rhodium salts.

Registry No. **1**, 33308-86-0; **3**, 137365-88-9; **4**, 137365-92-5; (η^1-Ind)Re(CO)$_3$[P(n-Bu)$_3$]$_2$, 93757-34-7; (η^1-Ind)Re(CO)$_3$[P(OPh)$_3$]$_2$, 137365-89-0; (η^1-Ind)Re(CO)$_3$(diphos), 137365-90-3; (η^1-Ind)Re(CO)$_3$[PCy$_3$]$_2$, 137365-91-4; (η^5-Ind)Re(CO)$_2$[P(OPh)$_3$], 137365-93-6; (η^5-Ind)Re(CO)$_2$[PCy$_3$], 137365-94-7; (η^5-TdH$_2$)Re(CO)$_3$, 121619-84-9; (η^1-TdH$_2$)Re(CO)$_3$[P(OEt)$_3$]$_2$, 137365-95-8; (η^1-TdH$_2$)Re(CO)$_2$[P(OEt)$_3$], 137365-96-9; (η^5-Td)[Re(CO)$_3$]$_3$, 121653-41-6; (η^1-Td)[Re(CO)$_3$[P(n-Bu)$_3$]$_2$]$_3$, 137393-40-9; (η^5-Td)[Re(CO)$_2$P(n-Bu)$_3$]$_3$, 137365-97-0; (η^5-Td)[Mn(CO)$_3$]$_3$, 121653-39-2; (η^5-Td)[Rh(CO)$_2$]$_3$, 137365-87-8; (η^5-Td)[Rh(CO)PPh$_3$]$_3$, 137365-98-1; (η^5-Td)[Rh(CO)P(n-Bu)$_3$]$_3$, 137365-99-2; [Rh(COD)Cl]$_2$, 12092-47-6; (η^5-Td)[Rh(COD)]$_3$, 137365-86-7; TdH$_3$, 73255-13-7; PCy$_3$, 2622-14-2; P(OPh)$_3$, 2622-14-2; P(OEt)$_3$, 122-52-1; PMePh$_2$, 1486-28-8; diphos, 1663-45-2; P(n-Bu)$_3$, 998-40-3; PMe$_2$Ph, 672-66-2; PMe$_3$, 594-09-2; (η^5-Cp)Rh(CO)$_2$, 12192-97-1; (η^5-Ind)Rh(CO)$_2$, 12153-10-5.

Supplementary Material Available: Derivations of the equations used to generate estimated simulated curves of spectral changes for reactions at the four different experimental conditions shown in Figure 1a–d (4 pages). Ordering information is given on any current masthead page.

(15) Walker, H. W.; Rattinger, G. B.; Belford, R. L.; Brown, T. L. *Organometallics* **1983**, *2*, 775.

Synthesis and Electronic Structure of Permethylindenyl Complexes of Iron and Cobalt

Dermot O'Hare,*[†] Jennifer C. Green,*[†] Todd Marder,*[‡] Scott Collins,[‡] Graham Stringer,[‡] Ashok K. Kakkar,[‡] Nikolas Kaltsoyannis,[†] Alexander Kuhn,[†] Rhian Lewis,[†] Christian Mehnert,[†] Peter Scott,[†] Mohamedally Kurmoo,[†] and Stuart Pugh[†]

Inorganic Chemistry Laboratory, South Parks Road, Oxford OX1 3QR, U.K., and Department of Chemistry, University of Waterloo, Waterloo, Ontario N2L 3G1, Canada

Received May 7, 1991

Fe(η^5-C$_9$Me$_7$)$_2$ and Co(η^5-C$_9$Me$_7$)$_2$ have been prepared by treatment of either FeCl$_2$·xTHF ($x \cong 2$) or Co(acac)$_2$ with LiInd* (Ind* = η^5-C$_9$Me$_7$) in THF. The cyclic voltammograms of both Fe(η^5-C$_9$Me$_7$)$_2$ and Co(η^5-C$_9$Me$_7$)$_2$ indicate that they are redox active with one-electron oxidations at $E_{1/2}$ = −0.32 and −1.05 V vs SCE, respectively; both complexes exhibit second oxidations at $E_{1/2}$ = 1.28 and 1.21 V vs SCE, respectively. The 17-electron and 18-electron cations [Fe(η^5-C$_9$Me$_7$)$_2$]$^+$PF$_6^-$ and [Co(η^5-C$_9$Me$_7$)$_2$]$^+$PF$_6^-$ were isolated by treatment of the neutral complexes with either [Fe(η^5-C$_5$H$_5$)$_2$]$^+$PF$_6^-$ (for Fe) or NH$_4$PF$_6$ (for Co). Gas-phase UV photoelectron spectroscopy experiments on both Fe(η^5-C$_9$Me$_7$)$_2$ and Co(η^5-C$_9$Me$_7$)$_2$ show that the permethylindenyl ligand gives rise to lower first ionization energy (correlating with a more negative $E_{1/2}$ value) than the Cp* (Cp* = η^5-C$_5$Me$_5$) ligand for Fe, while in the Co analogue the reverse is found. EPR and magnetic susceptibility experiments on [Fe(η^5-C$_9$Me$_7$)$_2$]$^+$PF$_6^-$ and Co(η^5-C$_9$Me$_7$)$_2$ both in solution and the solid state yield magnetic moments of 2.09 μ_B for [Fe(η^5-C$_9$Me$_7$)$_2$]$^+$PF$_6^-$ and 1.59 μ_B for Co(η^5-C$_9$Me$_7$)$_2$.

Introduction

Transition-metal indenyl compounds have attracted interest in recent years as an alternative to the cyclopentadienyl ligand for two main reasons. The relative ease of slippage of the indenyl ring from η^5 to η^3 coordination has been proposed to account for the enhanced reactivity in both S_N1[1-3] and S_N2[1-6] substitution reactions compared

[†] Inorganic Chemistry Laboratory.
[‡] University of Waterloo.

(1) O'Connor, J. M.; Casey, C. P. *Chem. Rev.* **1987**, *87*, 307.

0276-7333/92/2311-0048$03.00/0

to their cyclopentadienyl analogues ("the indenyl effect").[7] In addition, enhanced catalytic activity has been demonstrated for (η^5-indenyl)ML_2 complexes (M = Co, Rh; L = alkene) in intermolecular hydroacylation reactions,[8] cyclotrimerization of alkynes to benzenes,[9] and cyclotrimerization of alkynes and nitriles to pyridines.[10] In this paper we report on the synthesis of the permethylindenyl complexes $[M(\eta^5\text{-}C_9Me_7)_2]^{0/+}$ (M = Fe, Co) and a study of their electronic structures using gas-phase photoelectron spectroscopy, cyclic voltammetry, magnetic susceptibility, and EPR spectroscopy where appropriate. Comparisons are made with the electronic structure of the analogous cyclopentadienyl, pentamethylcyclopentadienyl, and indenyl derivatives. We have recently published a preliminary report on the synthesis and X-ray structure determinations of $Fe(\eta^5\text{-}C_9Me_7)_2$, $Fe(\eta^5\text{-}C_9H_7)_2$, $Co(\eta^5\text{-}C_9H_7)_2$, and $Ni(\eta^5\text{-}C_9H_7)_2$ in order to investigate the degree of slip–fold distortion in indenyl ligands as a function of d-electron count.[11] A brief description of the synthesis of permethylindene and $Fe(\eta^5\text{-}C_9Me_7)_2$ has previously appeared[12] but few details were provided.

Experimental Section

General Procedures. All reactions were performed by using standard Schlenk techniques or in a Vacuum Atmospheres Dri-Box under a nitrogen atmosphere. NMR spectra were recorded using Bruker AM300 (300 MHz) or AC200 (200 MHz) spectrometers. All samples were prepared under nitrogen and were placed in airtight screw top tubes or sealed under vacuum. The spectra were referenced using solvent peaks as internal standards. All chemical shifts are in ppm, relative to δ (tetramethylsilane) = 0 ppm. Solvents were predried over molecular sieves (type 4 Å) and refluxed with rigorous drying agents under a continuous stream of nitrogen. THF and diethyl ether were refluxed over sodium/potassium alloy, and CS_2 was refluxed over CaH_2. Solvents were distilled prior to use and were stored over molecular sieves in flame-dried ampules under nitrogen.

Equipment. Cyclic voltammograms were recorded in the three-electrode configuration with a platinum-disk working electrode, platinum-gauze auxiliary electrode, and a silver-wire pseudoreference electrode in acetonitrile/0.1 M $[N(Bu^n)_4]^+[PF_6]^-$. All potentials were referenced to the saturated calomel electrode by measuring the ferrocene/ferrocenium couple ($E_{1/2}$ = 0.41 V vs SCE) under the same conditions or by addition of a small amount of ferrocene as an internal standard.

The gas-phase ultraviolet photoelectron spectra were measured using a PES Laboratories 0078 spectrometer interfaced with a Research Machines 380Z microcomputer. Both He I and He II radiation were used for spectral acquisition. Data were collected by repeated scans and the spectra calibrated with He, Xe, and N_2. Relative band areas were found normalized to those of the first band; the He II/He I intensity ratios, expressed as $R_{2/1}$ values are given in Table III.

Solution magnetic susceptibility measurements were performed on a Bruker AM 300 spectrometer using the Evans method,[13] and typically $[Fe(\eta^5\text{-}C_9Me_7)_2]^+PF_6^-$ (12 mg, 0.019 mmol) or $Co(\eta^5\text{-}C_9Me_7)_2$ (15 mg, 0.019 mmol) was dissolved in either CD_2Cl_2 or $C_6D_5CD_3$ (0.5 cm^3) with 1% TMS. Solid-state magnetic susceptibility measurements were carried out using microcrystalline samples and a Faraday balance at Central Research and Development, E. I. du Pont de Nemours, Wilmington, DE; details of the experimental setup can be found elsewhere.[14] The susceptibilities have been corrected for the intrinsic diamagnetism of the sample container and the diamagnetism of the electronic cores of the constituent atoms (χ_{dia} = 375 × 10^{-6} emu mol^{-1} for **2**).

EPR spectra were obtained using the X-band of a Bruker ESP-300 spectrometer. The samples were prepared under nitrogen as CH_2Cl_2 or THF solutions and run in 4-mm high-purity Spectosil quartz tubes fitted with a Young's Teflon stopcock.

Elemental microanalyses were performed by the Analytical Services of the Inorganic Chemistry Laboratory or in the case of **3** by Analytische Laboratorien, Postfach 135, Engelskirchen, Germany.

Heptamethylindene (C_9Me_7H).[12] Tiglic acid (50 g, 0.5 mol) was mixed with thionyl chloride (500 mL) and the mixture refluxed for 5 h. Excess thionyl chloride was evaporated off at 78 °C. Distillation of the product under reduced pressure (10 mmHg, ca. 37 °C) gave a colorless liquid (tigloyl chloride) in 95% yield.

To a stirring mixture of $AlCl_3$ (105 g, 0.8 mol) in CS_2 (500 cm^3) at −5 °C, a mixture of 1,2,3,4-tetramethylbenzene (100 g, 0.75 mol) and tigloyl chloride (87 g, 0.75 mol) was added slowly over a period of 1 h. After the addition, the mixture turned red-brown and solid CS_2 (300 mL) was added; the mixture was warmed to room temperature and stirred overnight. It was then heated at 50 °C for 2 h and finally poured onto a mixture of ice (1 kg) and concentrated HCl (1 L). The mixture was then extracted in diethyl ether and the ether layer dried over $CaCl_2$. On distillation, a dark brown crude liquid was obtained, which was further distilled under reduced pressure giving a yellow oily liquid (2,3,4,5,6,7-hexamethylindan-1-one ketone) in 85% yield.

The ketone (115 g, 0.58 mol) was dissolved in ether (500 cm^3), and LiMe (400 cm^3 of a 1.4 M solution in ether) was added dropwise at ice temperature. The mixture was then refluxed overnight. It was quenched with a saturated solution of ammonium chloride (1 L). The ether layer was dried over sodium sulfate. After filtration, the ether was removed in vacuo. Iodine (0.55 g) was added to the yellow oily liquid, and it was heated at 100 °C for 1 h. The dark brown product was extracted in ether. The ether layer was washed with water, 10% $Na_2S_2O_4$ solution, and finally water again. The extract was dried with sodium sulfate and then column-chromatographed on silica using petroleum ether (bp 40/60 °C) as the eluent. A bright yellow band was collected, which on removal of the solvent gave a light yellow solid of heptamethylindene in 80% yield (90 g). ^{1}H NMR ($CDCl_3$): δ 3.17 (q, 1 H), 2.5 (s, 3 H), 2.31 (s, 3 H), 2.22 (s, 6 H), 1.94 (s, 3 H), 1.23 (d, 3 H). ^{13}C NMR ($CDCl_3$, 50.3 MHz): δ 144.7, 142.4, 140.6, 133.6, 131.8, 130.4, 128.0, 126.1, 46.1, 16.3, 16.0, 15.9, 15.6, 15.0, 11.9. Infrared spectra (thin film): 2923, 2853, 1463, 1377 cm^{-1}.

Lithium Heptamethylindenide ($Li^+[C_9Me_7]^-$, Li(Ind*)). Heptamethylindene (17.5 g, 0.081 mol) was dissolved in petroleum ether (bp 40/60 °C; 100 cm^3) together with tetramethyl-

(2) White, C.; Mawby, R. J. *Inorg. Chim. Acta* **1970**, *4*, 261.
(3) Turaki, N. N.; Huggins, J. M.; Lebioda, L. *Inorg. Chem.* **1988**, *27*, 424.
(4) Caddy, P.; Green, M.; O'Brien, E.; Smart, L. E.; Woodward, P. *J. Chem. Soc., Dalton Trans.* **1980**, 962.
(5) Ji, L. N.; Rerek, M. E.; Basolo, F. *Organometallics* **1984**, *3*, 740.
(6) Kakkar, A. K.; Taylor, N. J.; Marder, T. B. *Organometallics* **1989**, *8*, 1765.
(7) Rerek, M. E.; Basolo, F. *J. Am. Chem. Soc.* **1984**, *106*, 5908.
(8) Marder, T. B.; Roe, D. C.; Milstein, D. *Organometallics* **1988**, *7*, 1451.
(9) Caddy, P.; Green, M.; Smart, L. E.; White, N. *J. Chem. Soc., Chem. Commun.* **1978**, 839. Borrini, A.; Diversi, P.; Ingroisso, G.; Lucherini, A.; Serra, G. *J. Mol. Catal.* **1985**, *30*, 181.
(10) Bonneman, H. *Angew. Chem., Int. Ed. Engl.* **1985**, *24*, 248. Bonneman, H.; Brijoux, W. In *Aspects of Homogeneous Catalysis*; Ugo, R., Ed.; D. Riedel: Dordrecht, The Netherlands, 1984; Vol. 5, 75.
(11) Westcott, S. A.; Kakkar, A. K.; Stringer, G.; Taylor, N. J.; Marder, T. B. *J. Organomet. Chem.* **1990**, *394*, 777.
(12) Miyamoto, T. K.; Tsutsui, M.; Chen, L. B. *Chem. Lett.* **1981**, 729.
(13) Deutsch, J. L.; Poling, S. M. *J. Chem. Educ.* **1969**, *46*, 167.
(14) Ward, M. D.; Fagan, P. J.; Calabrese, J. C.; Johnson, D. C. *J. Am. Chem. Soc.* **1989**, *111*, 1719.
(15) Evans, S.; Green, M. L. H.; Jewitt, B.; Orchard, A. F.; Pygall, C. F. *J. Chem. Soc., Faraday Trans. 2* **1972**, *68*, 1847.
(16) Cauletti, C.; Green, J. C.; Kelly, R.; Powell, P.; J. V. T., Robbins, J.; Smart, J. *J. Elect. Spectrosc. Relat. Phenom.* **1980**, *19*, 327.
(17) Crossley, N. S.; Green, J. C.; Nagy, A.; Stringer, G. *J. Chem. Soc., Dalton Trans.* **1989**, 2139.
(18) Warren, K. D. *Inorg. Chem.* **1974**, *13*, 1317.
(19) Warren, K. D. *Struct. Bonding (Berlin)* **1976**, *27*, 45.
(20) Prins, R. *Mol. Phys.* **1970**, *19*, 603.
(21) Ammeter, J. H. *J. Magn. Reson.* **1978**, *30*, 299.
(22) Evans, D. F. *J. Chem. Soc.* **1959**, 2003.
(23) Robbins, J. L.; Edelstein, N.; Spencer, B.; Smart, J. C. *J. Am. Chem. Soc.* **1982**, *104*, 1882.
(24) Koelle, U.; Khouzami, F. *Angew. Chem., Int. Ed. Engl.* **1980**, *19*, 640.
(25) Treichel, P. M.; Johnson, J. W.; Wagner, K. P. *J. Organomet. Chem.* **1975**, *88*, 227.

ethylenediamine (TMEDA; 1–2 cm³). LiBuⁿ (40 cm³ of a 2.5 M solution in hexane, 0.1 mol) was added dropwise. A white precipitate was produced immediately; the reaction mixture was stirred for 1 h, filtered, washed twice with petroleum ether (bp 40/60 °C; 2 × 100 cm³), and dried in vacuo. Yield: 18.0 g, 95%.

Bis(heptamethylindenyl)iron(II) ($Fe(\eta^5\text{-}C_9Me_7)_2$ (1)).[12] Lithium heptamethylindenide (9.5 g, 0.043 mol) was dissolved in THF (200 mL) to give a light brown solution. $FeCl_2 \cdot x$THF ($x \cong 2$) (3.3 g, ca. 0.012 mol) was suspended in THF (50 cm³). Slow addition of the lithium salt to the $FeCl_2 \cdot x$THF suspension gave a deep purple-black solution. After the solution was stirred for 2 h, purple crystals appeared on the side of the flask. The solvent was removed under reduced pressure, and the resulting black residue was extracted with hexane (2 × 50 cm³), giving a purple solution. The solution was concentrated to ca. 30 cm³, and cooling to −40 °C gave black crystals of $Fe(\eta^5\text{-}C_9Me_7)_2$. Yield: 51.1%, 5.5 g. Anal. Found (calc) for $C_{32}H_{42}Fe$: C, 79.93 (79.65); H, 8.82 (8.77); Fe, 11.60 (11.57). ^1H NMR (C_6D_6): δ 1.70 (s, 2 × Me), 1.95 (s, 4 × Me), 2.15 (s, 4 × Me), 2.32 (s, 4 × Me). ^{13}C NMR (C_6D_6, 50.3 MHz): δ 130.6, 128.9, 85.5, 85.3, 70.8, 17.5, 16.9, 12.5, 10.3.

Bis(heptamethylindenyl)iron(III) Hexafluorophosphate ($[Fe(\eta^5\text{-}C_9Me_7)_2]^+[PF_6]^-$ (2)). To a solution of $Fe(\eta^5\text{-}C_9Me_7)_2$ (0.77 g, 1.6 mmol) in THF was added dropwise a solution of $[Fe(\eta^5\text{-}C_5H_5)_2]^+PF_6^-$ (0.49 g, 1.5 mmol) in acetonitrile. The mixture was stirred for ca. 5 h. The solvents were removed under reduced pressure, and the remaining brown solid was washed with toluene (2 × 30 cm³) and then diethyl ether (2 × 30 cm³) to remove the ferrocene byproduct. The resulting purple-brown residue was recrystallized from CH_2Cl_2 overnight, giving black crystals. Yield: 75%. Anal. Found (calc) for $C_{32}H_{42}FePF_6$: C, 61.33 (61.24); H, 6.90 (6.70); Fe, 8.80 (8.93). ^1H NMR (CD_2Cl_2): 34.75 br s, 20.43 br s, −16.59 br s.

Bis(heptamethylindenyl)cobalt(III) Hexafluorophosphate ($[Co(\eta^5\text{-}C_9Me_7)_2]^+[PF_6]^-$ (3)). To a suspension of $Co(acac)_2$ (1.05 g, 4.09 mmol) in THF (50 cm³) was added a solution of lithium heptamethylindenide (1.82 g, 8.18 mmol) in THF (40 cm³). The resultant light brown mixture was stirred for 2 h at room temperature. The volatiles were then removed under reduced pressure, and the resulting black residue was extracted with petroleum ether (bp 40/60 °C; 2 × 50 cm³), giving a dark red solution. The solution was filtered through a bed of Celite. A saturated solution of NH_4PF_6 in THF (ca. 10 cm³) was added to the petroleum ether solution. A bright red floculant precipitate formed immediately, which was collected on a frit and washed with degassed water (2 × 10 cm³) to dissolve the unreacted NH_4PF_6. The precipitate was dried in vacuo for ca. 12 h and recrystallized from a 1:1 acetone/diethyl ether mixture at −20 °C, yielding dark red crystals of $[Co(\eta^5\text{-}C_9Me_7)_2]^+[PF_6]^-$. Yield: 47% (1.2 g; 1.9 mmol). ^1H NMR ($(CD_3)_2CO$): δ 2.39 (s, 4 Me), 2.36 (s, 4 Me), 2.04 (s, 2 Me), 1.92 (s, 4 Me). ^{13}C NMR ($(CD_3)_2CO$): δ 140 (s, 4 C), 129 (s, 4 C), 102 (s, 2 C), 97 (s, 4 C), 87 (s, 4 C), 19 (q, 8 Me), 11 (q, 4 Me), 9 (q, 2 Me). IR (Nujol): 2924, 2854, 1463, 1378, 1201, 801 cm⁻¹. Anal. Found (calc) for $CoC_{32}H_{42}PF_6$: C, 60.47 (60.96); H, 6.73 (6.70); Co, 9.54 (9.35).

Bis(heptamethylindenyl)cobalt(II) ($Co(\eta^5\text{-}C_9Me_7)_2$ (4)). An analytically pure sample of $Co(\eta^5\text{-}C_9Me_7)_2$ could not be isolated by recrystallization of the petroleum ether fraction above. However, we were able to prepare a pure sample by reduction of $[Co(\eta^5\text{-}C_9Me_7)_2]^+[PF_6]^-$. A suspension of $[Co(\eta^5\text{-}C_9Me_7)_2]^+[PF_6]^-$ (0.26 g, 0.41 mmol) in THF (30 cm³) was added to a 1% sodium amalgam (ca. 100 g), and the reaction mixture was stirred for 3 h. A clear dark red solution was obtained. The unreacted sodium amalgam was removed by filtering the reaction mixture through a bed of Celite. Removal of the solvent under reduced pressure gave a dark red residue, which was extracted with toluene (2 × 50 cm³). The solution was concentrated to ca. 30 cm³, and on slow cooling to −20 °C gave bright red crystals of $Co(\eta^5\text{-}C_9Me_7)_2$ in 43% yield (0.085 g; 0.17 mmol). Anal. Found (calc) for $CoC_{32}H_{42}$: C, 79.10 (79.14); H, 8.60 (8.71). ^1H NMR (C_6D_6): δ 7.03 (s, br). IR (Nujol): 2931, 2855, 1463, 1377, 1019, 801 cm⁻¹. Solution magnetic moment (Evans method): $\mu_{eff} = 1.49 \pm 0.2\ \mu_B$.

Results and Discussion

Synthesis and Characterization of $[M(\eta^5\text{-}C_9Me_7)_2]^{0/+}$ (M = Fe, Co). Synthesis. Reaction of anhydrous $FeCl_2 \cdot x$THF ($x \cong 2.0$) with the lithium salt of heptamethylindene gives $[Fe(\eta^5\text{-}C_9Me_7)_2]$[12] (1), a black, volatile, air-sensitive crystalline compound readily soluble in hydrocarbon solvents. Although the synthesis of the ligand heptamethylindene (Ind*H) is a multistep reaction (Scheme I), it can be prepared in large quantities (ca. 20–30 g) in 50% overall yield starting from relatively inexpensive tiglic acid and 1,2,3,4-tetramethylbenzene. Compound 1 can be quantitatively oxidized to the 17-electron radical-cation $[Fe(\eta^5\text{-}C_9Me_7)_2]^+[PF_6]^-$ (2) by addition of ferrocenium hexafluorophosphate in THF (Scheme II). The resultant purple-black precipitate can be recrystallized from CH_2Cl_2 to give black analytically pure cuboidal crystals. Unfortunately, we have not yet obtained large enough single crystals for an X-ray structure determination.

Scheme I[a]

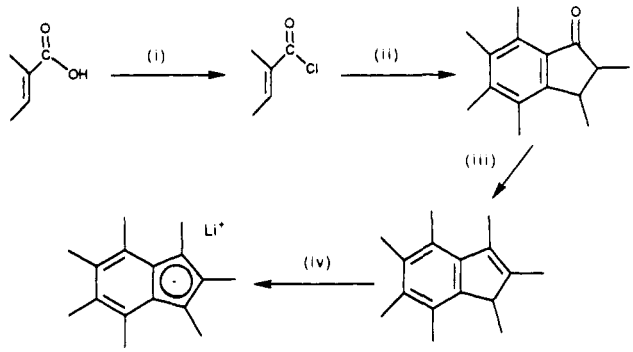

[a] Key: (i) SO_2Cl_2, reflux, 95%; (ii) 1,2,3,4-tetramethylbenzene, $AlCl_3$, CS_2, 85%; (iii) LiMe, Et_2O, and then I_2 reflux, 80%; (iv) $LiBu^n$ in Et_2O, 90%.

Table I. Electrochemical Oxidation Potentials of Selected Metallocenes

compd	oxidn potential (vs SCE), V	ref	1st IE, eV	ref
$[Co(\eta\text{-}C_5Me_5)_2]^{+/0}$	-1.47	23	4.70	16
$[Co(\eta\text{-}C_9Me_7)_2]^{+/0}$	-1.05	this work	4.89	this work
$[Co(\eta\text{-}C_5H_5)_2]^{+/0}$	-0.91	24	5.55	16
$[Fe(\eta\text{-}C_9Me_7)_2]^{+/0}$	-0.32	this work	5.54	this work
$[Fe(\eta\text{-}C_5Me_5)_2]^{+/0}$	-0.12	23	5.88	15
$[Fe(\eta\text{-}C_9H_7)_2]^{+/0}$	+0.13	25	6.50	17
$[Fe(\eta\text{-}C_5H_5)(\eta\text{-}C_9H_7)]^{+/0}$	+0.27	25		
$[Fe(\eta\text{-}C_5H_5)_2]^{+/0}$	+0.41	23	6.86	16

Treatment of freshly sublimed $Co(acac)_2$ with LiInd* ($Li^+C_9Me_7^-$) in THF gives $Co(\eta^5\text{-}C_9Me_7)_2$ (3). Although is not possible to isolate an analytically pure sample of 3 from this reaction mixture, oxidation of the reaction mixture with NH_4PF_6 gave a red precipitate of $[Co(\eta^5\text{-}C_9Me_7)_2]^+[PF_6]^-$ (4). Reduction of 4 with 1% sodium amalgam in THF yielded 3 in high purity. Compound 3 is bright red and thermally stable but oxygen sensitive.

Electrochemical Experiments. The cyclic voltammograms of 2 and 4 in dry oxygen-free acetonitrile both show facile reversible M^+/M^+ redox couples at −0.32 and −1.05 V, respectively. Table I gives these half-wave potentials ($E_{1/2}$) together with those for the corresponding cyclopentadienyl and pentamethylcyclopentadienyl analogues for comparison. For both 1 and 3, the trend in oxidation potential mirrors that of the gas-phase first ionization energies. These trends are discussed in relation to the photoelectron spectra (vide infra).

Unexpectedly, both 1 and 3 show a second reversible oxidation at +1.28 and +1.21 V vs SCE, respectively.

Scheme II[a]

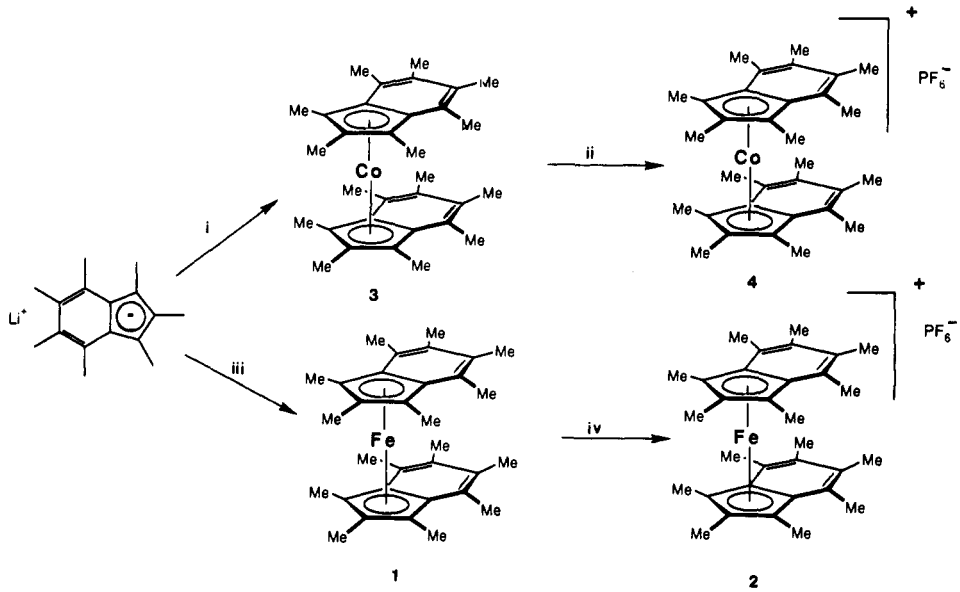

[a] Key: (i) $Co(acac)_2$ in THF, 43%; (ii) NH_4PF_6, 90%; (iii) $FeCl_2 \cdot x$THF ($x \cong 2$) in THF, 51%; (iv) $Fe(C_5H_5)_2^+PF_6^-$, 85%.

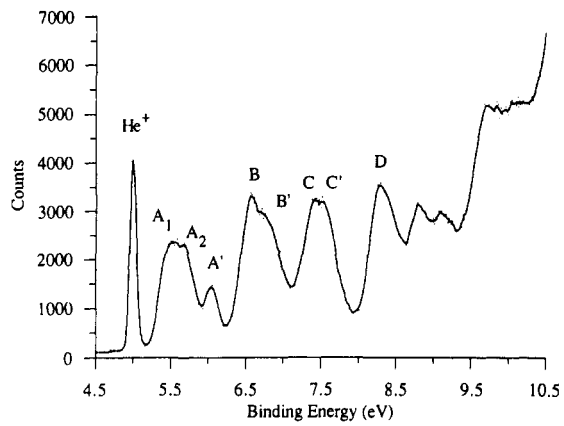

Figure 1. Low ionization energy region of the He I photoelectron spectrum of $Fe(\eta^5\text{-}C_9Me_7)_2$.

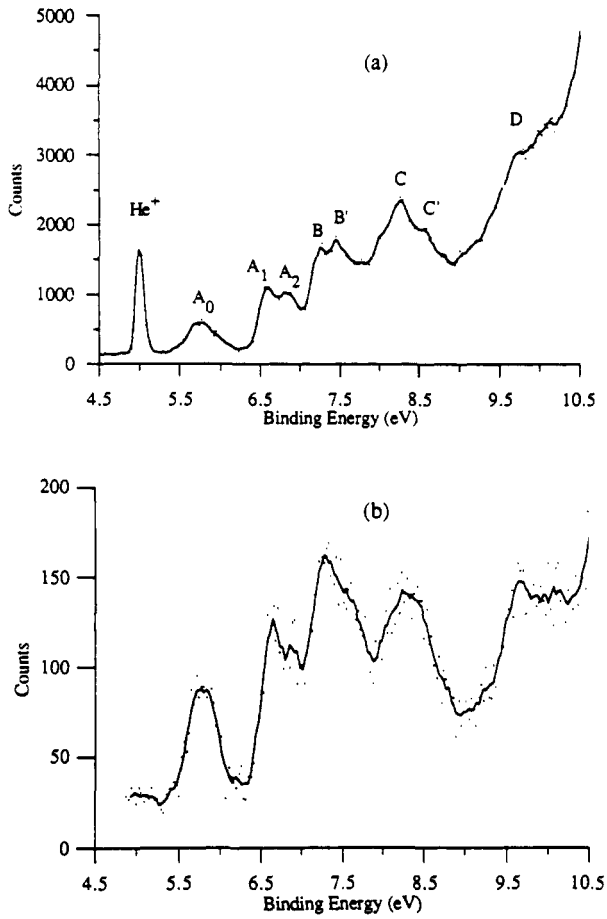

Figure 2. Low ionization energy region of the (a) He I and (b) He II photoelectron spectra of $Co(\eta^5\text{-}C_9H_7)_2$.

Consequently, it may be possible to prepare chemically these dicationic species $[M(\eta^5\text{-}C_9Me_7)_2]^{2+}[PF_6^-]_2$. We are currently investigating this possibility. We believe that decamethylferrocene is the only other 18-electron metallocene to undergo two reversible oxidations. In the latter case this second oxidation was observed at $E_{1/2} = 1.39$ V (vs Al electrode) in $AlCl_3$/1-butylpyridinium chloride melts containing an excess of $AlCl_3$.[26]

Photoelectron Spectroscopy. The He I photoelectron (PE) spectrum of $Fe(\eta^5\text{-}C_9Me_7)_2$ is presented in Figure 1, and Figures 2 and 3 give the He I and He II spectra of both $Co(\eta^5\text{-}C_9H_7)_2$ and $Co(\eta^5\text{-}C_9Me_7)_2$. The points in the spectra represent the experimental data, and the continuous line represents a least-squares fit to these points. Ionization energy (IE) data are collected in Table II together with IE data for $Fe(\eta^5\text{-}C_5H_5)_2$,[15] $Fe(\eta^5\text{-}C_5Me_5)_2$, $Co(\eta^5\text{-}C_5H_5)_2$, $Co(\eta^5\text{-}C_5Me_5)_2$,[16] and $Fe(\eta^5\text{-}C_9H_7)_2$[17] for comparative purposes.

General Bonding Model. In general, the bonding in the indenyl compounds will resemble that of the analogous cyclopentadienyl compounds, which have already been the subject of molecular orbital (MO) calculations and photoelectron spectroscopic (PES) studies.[15,16] The He I and He II PE spectra of $Fe(\eta^5\text{-}C_9H_7)_2$ and their interpretation in terms of an MO scheme for these systems have already been discussed.[17] Figure 4 presents qualitative MO schemes for $Fe(\eta^5\text{-}C_9Me_7)_2$ and $Co(\eta^5\text{-}C_9H_7)_2$ with orbital labelings corresponding to the PE spectra in Figures 1 and

(26) Gale, R. J.; Osteryoung, R. A. *Inorg. Chem.* **1979**, *18*, 1603. Gale, R. J.; Gilbert, B.; Osteryoung, R. A. *Ibid.* **1979**, *18*, 2723.

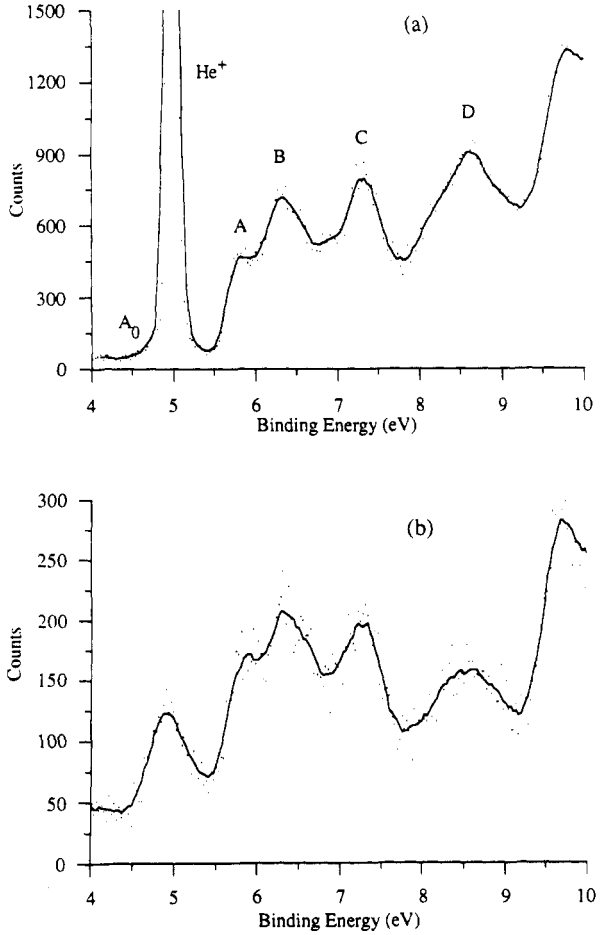

Figure 3. Low ionization energy region of the (a) He I and (b) He II photoelectron spectra of $Co(\eta^5\text{-}C_9Me_7)_2$.

2. The MO diagram for $Co(\eta^5\text{-}C_9Me_7)_2$ will be closely related to those given in the figure.

Figure 5 shows the projection onto the xy plane of the indenyl π orbitals, five of which are filled in the anion. The three highest lying occupied π MOs, π_5, π_4, and π_3 resemble the degenerate e_1 HOMO of the cyclopentadienyl anion, having one nodal plane cutting through the C_5 ring and, as such, might be expected to interact with the d_{xz} and d_{yz} orbitals of the metal fragment. Such interaction will be greater for π_5 than π_3, as π_5 has greater localization on the C_5 ring than π_3, gives bigger overlap, and also lies closer in energy to the metal d orbitals. One important distinction between π_5 and the analogous $[C_5H_5]^-$ orbitals is that is has very little density on the bridgehead atoms 8 and 9 of the five-membered ring.

In the bis(indenyl) complexes, assuming C_{2v} symmetry, the π orbitals of the two indenyl fragments may be combined in symmetric and antisymmetric combinations with respect to the mirror plane, xy. Calculations predict mixing of the d_{xy} orbital with the symmetric combination of the two π_5 orbitals of b_1 symmetry.[17] The antisymmetric combination of the two π_5 orbitals combines with d_{yz}. The principal interaction of the π_4 orbitals is with the d_{xz} orbital. The π_3 orbitals are thought to be less involved in bonding.

Assignment of the PE Spectra. The PE spectrum of $Fe(\eta^5\text{-}C_9Me_7)_2$ is readily assigned by comparison with the PE spectrum of $Fe(\eta^5\text{-}C_9H_7)_2$.[17] Band A_1 is assigned to ionization from the d_{xy} orbital, which is mixed in an antibonding manner with π_5, band A_2 to the $d_{x^2-y^2}$ orbital, and A′ to the d_{z^2} orbital. These three orbitals are primarily metal localized. Bands B and B′ are assigned to π_5 combined with d_{xz} and d_{yz}, respectively. Bands C and C′ relate to orbitals largely localized on π_4, and band D relates to π_3 ionizations.

Table II. Ionization Energies and Assignments for $Fe(\eta^5\text{-}C_9Me_7)_2$, $Fe(\eta^5\text{-}C_9H_7)_2$, $Fe(\eta^5\text{-}C_5Me_5)_2$, $Fe(\eta^5\text{-}C_5H_5)_2$, $Co(\eta^5\text{-}C_9Me_7)_2$, $Co(\eta^5\text{-}C_9H_7)_2$, $Co(\eta^5\text{-}C_5H_5)_2$, and $Co(\eta^5\text{-}C_5Me_5)_2$

compd	band	IE, eV	assgnt
$Fe(\eta^5\text{-}C_9Me_7)_2$	A_1	5.54	$d_{xy} - \pi_5$
	A_2	5.72	$d_{x^2-y^2}$
	A′	6.18	d_{z^2}
	B	6.70	$\pi_5 + d_{xy}$
	B′	6.93	$\pi_5 + d_{yz}$
	C		
	C′	7.72	π_4, $d_{xz} + \pi_4$
	D	8.65	$\pi_3 \times 2$
		9.17	
		9.50	
		10.19	
		10.52	
		11.80	
		13.22	
$Co(\eta^5\text{-}C_9H_7)_2$	A_0	5.82	$d_{xz} - \pi_4$
	A_1	6.72	
	A_2	6.92	$d_{xy} - \pi_5$, $d_{x^2-y^2}$, d_{z^2}
	B	7.42	
	B′	7.61	$\pi_5 + d_{xy}$, $\pi_5 + d_{yz}$
	C	8.48	
	C′	8.80	π_4, $d_{xz} + \pi_4$
	D	10.0	$\pi_3 \times 2$
$C(\eta^5\text{-}C_9Me_7)_2$	A_0	4.89	$d_{xz} - \pi_4$
	A	5.89	
	B	6.37	$d_{xy} - \pi_5$, $d_{x^2-y^2}$, d_{z^2}, $\pi_5 + d_{xy}$, $\pi_5 + d_{yz}$
	C	7.49	π_4, $d_{xz} + \pi_4$
	D	8.89	$\pi_3 \times 2$
$Fe(\eta^5\text{-}C_9H_7)_2$		6.5	$d_{xy} - \pi_5$
		6.65	$d_{x^2-y^2}$
		6.97	d_{z^2}
		7.89	$\pi_5 + d_{xy}$
		8.10	$\pi_5 + d_{yz}$
		8.90	π_4, $\pi_4 + d_{xz}$
		9.96	$\pi_3 \times 2$
$Fe(\eta^5\text{-}C_5H_5)_2$		6.86	$^2E_{2g}$
		7.21	$^2A_{1g}$
		8.77	$^2E_{1u}$
		9.28	$^2E_{1g}$
$Fe(\eta^5\text{-}C_5Me_5)_2$		5.88	$^2E_{2g}$
		6.28	$^2A_{1g}$
		7.31	$^2E_{1u}$
		8.08	$^2E_{1g}$
$Co(\eta^5\text{-}C_5H_5)_2$		5.55	$^1A_{1g}$
		7.15	$^3E_{1g}$
		7.65	$^3E_{2g}$
		7.99	$^1E_{2g}$
		8.72	ligand π + $^1E_{1g}$, $^3E_{1g}$
		9.92	$^1E_{1g}$
$Co(\eta^5\text{-}C_5Me_5)_2$		4.71	$^1A_{1g}$
		6.39	$^3E_{1g}$ + $^3E_{2g}$
		7.55	
		8.30	$^1E_{1g}$, $^3E_{1g}$, $^1E_{1g}$, $^1E_{2g}$ + ligand π

Assignment of the PE spectra of $Co(\eta^5\text{-}C_9H_7)_2$ and $Co(\eta^5\text{-}C_9Me_7)_2$ presents more difficulty than that of $Fe(\eta^5\text{-}C_9Me_7)_2$. $Co(\eta^5\text{-}C_9H_7)_2$ and $Co(\eta^5\text{-}C_9Me_7)_2$ are open-shell molecules, and the correlation between a single band in the PE spectrum and ionization from one MO no longer applies. A variety of ion states may be produced upon ionization from a single MO; in $Co(\eta^5\text{-}C_5H_5)_2$, for example, ionization from the predominantly d-based MOs leads to the formation of seven ion states (four singlet and three triplet).[16] Ligand field calculations reveal that ionization to triplet states requires lower energy than that to singlet states and that the energies of ionization to certain singlet states will be close to those of ligand-based ionizations. In $Co(\eta^5\text{-}C_5H_5)_2$, only five d bands are resolved, and in Co-

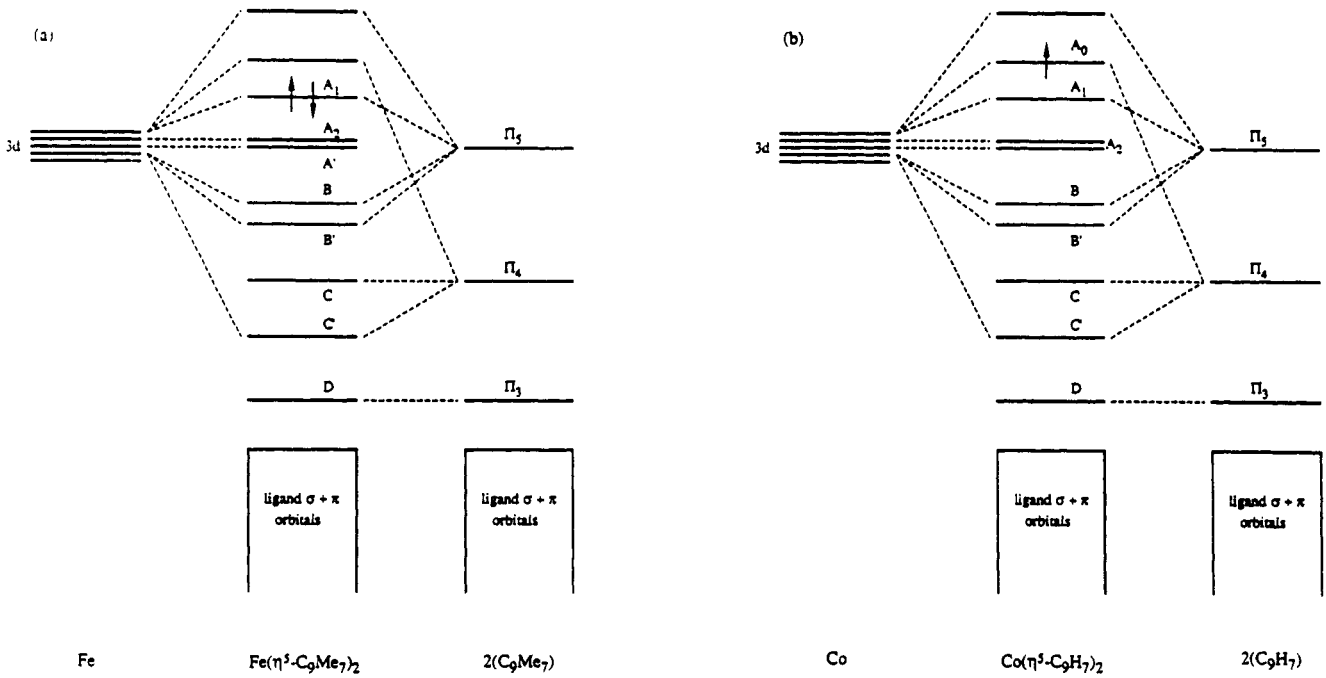

Figure 4. Qualitative molecular orbital diagrams for (a) $Fe(\eta^5\text{-}C_9Me_7)_2$ and (b) $Co(\eta^5\text{-}C_9H_7)_2$.

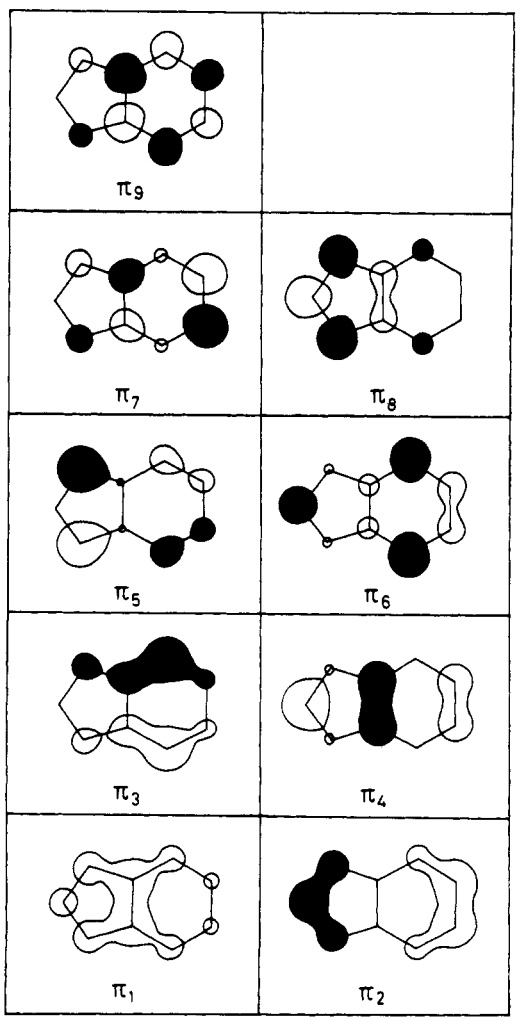

Figure 5. Projection onto the xy plane of the indenyl π orbitals.

$(\eta^5\text{-}C_5Me_5)_2$, only three can be distinguished. Permethylation lowers the IE of all PE bands but has more effect upon bands originating from orbitals with high lig- and character than those with high metal character and thus exacerbates the problem of d-band assignment.

The first band (band A_0) in the spectrum of $Co(\eta^5\text{-}C_9H_7)_2$ is assigned to ionization from an MO that is unoccupied in $Fe(\eta^5\text{-}C_9H_7)_2$ and $Fe(\eta^5\text{-}C_9Me_7)_2$—an antibonding combination of ligand π_4 and metal d_{xz} orbitals. Between ionization energies of 6.5 and 10.0 eV (bands A–D) the spectrum is less well resolved than the corresponding region in the $Fe(\eta^5\text{-}C_9Me_7)_2$ spectrum for the reasons outlined above. Bands C and D may be assigned in a manner analogous to those of $Fe(\eta^5\text{-}C_9Me_7)_2$, i.e. to the largely ligand-based π_4 and π_3 orbitals, respectively. Precise assignment of the bands labeled A_1, A_2, B, and B′ is not possible. There will certainly be peaks due to ionization of metal d electrons and also from the MOs derived from the mixing of the ligand π_5 orbitals with d_{xy} and d_{yz}. Meaningful $R_{2/1}$ (He II/He I intensity ratio) values are difficult to obtain due to the unresolved nature of the spectrum in this IE region, but the He II spectrum shows that bands A_0–B all increase in intensity relative to bands C and D, revealing a substantial metal contribution to the ionizing MOs. Band B′ falls away in the He II spectrum, suggesting that it arises from a more ligand-based MO. It would appear that four of the expected seven Co 3d based ionizations can be identified (bands A_0–B), although unequivocal assignment is not possible. Given that the d-band structure of $Fe(\eta^5\text{-}C_9H_7)_2$ closely resembles that of ferrocene, it seems probable that bands A_1 and A_2 in the spectrum of $Co(\eta^5\text{-}C_9H_7)_2$ and band A in that of $Co(\eta^5\text{-}C_9Me_7)_2$ arise from triplet ion states as is found in $Co(\eta^5\text{-}C_5R_5)_2$.

The spectrum of $Co(\eta^5\text{-}C_9Me_7)_2$ may be assigned in a manner analogous to that of $Co(\eta^5\text{-}C_9H_7)_2$, although the low-IE region is even less well resolved than that of $Co(\eta^5\text{-}C_9H_7)_2$ because of the effects of permethylation. Band A_0 is obscured by the He self-ionization peak in the He I spectrum but is clearly visible in the He II spectrum.

Comparison with Other Fe and Co Sandwich Compounds. The shifts in IE found on permethylating the indenyl ligands are given in Table III, together with the $R_{2/1}$ values for $Fe(\eta^5\text{-}C_9Me_7)_2$. The greater effect of permethylation on ligand-based ionizations is clearly illus-

Table III. Shifts in IE of Bands A–D on Permethylation of $Fe(\eta^5\text{-}C_9H_7)_2$ and $Co(\eta^5\text{-}C_9H_7)_2$ and $R_{2/1}$ Values for the PE Bands of $Fe(\eta^5\text{-}C_9Me_7)_2$

	band	shift	$R_{2/1}$
$Fe(\eta^5\text{-}C_9H_7)_2$	A_1	0.96	1.0
	A_2	0.93	1.0
	A′	0.89	1.4
	B	1.19	0.68
	B′	1.17	0.68
	C	1.18	0.54
	D	1.30	0.60
$Co(\eta^5\text{-}C_9H_7)_2$	A_0	0.93	
	A_1[a]	0.83	
	C and C′[b]	1.15	
	D	1.11	

[a] Compared with band A in $Co(\eta^5\text{-}C_9Me_7)_2$. [b] Shift of the average value of C and C′.

trated. The difficulty of correlating bands A_2, B, and B′ in the spectrum of $Co(\eta^5\text{-}C_9H_7)_2$ with the equivalent region of $Co(\eta^5\text{-}C_9Me_7)_2$ prevents many shift values from being obtained, although the shifts in bands A_1, C, and D are similar to those found for the Fe analogues. There is a strong link between IE shift and $R_{2/1}$ values in the Fe spectra—the higher the $R_{2/1}$ value, the higher the d character of the MO from which ionization is taking place. Similar effects are found on permethylation of ferrocene and cobaltocene.[16] The combined effect of indenyl substitution and methylation gives $Fe(\eta^5\text{-}C_9Me_7)_2$ a rather similar first IE to that of cobaltocene.[16]

Replacing the cyclopentadienyl ligands with indenyl ligands in the Fe case causes the first IE to drop by 0.36 eV. A 0.34-eV decrease is observed between the equivalent permethylated complexes. Indenyl and permethylindenyl can therefore be regarded as more electron donating than cyclopentadienyl and permethylcyclopentadienyl, respectively, in these d^6 compounds. This is in accord with the X-ray photoelectron spectroscopy studies of a series of Ru compounds containing the cyclopendadienyl, permethylcyclopentadienyl, and indenyl ligands,[27] in which shifts in the binding energy of the Ru $3d_{5/2}$ core level indicated that the electron-donating ability of the ligands decreased in order Cp* > Ind > Cp. In the d^7 Co systems, however, the reverse is found, the first IE increasing from 5.55 eV in $Co(\eta^5\text{-}C_5H_5)_2$ to 5.82 eV in $Co(\eta^5\text{-}C_9H_7)_2$ and from 4.71 eV in $Co(\eta^5\text{-}C_5Me_5)_2$ to 4.89 eV in $Co(\eta^5\text{-}C_9Me_7)_2$. This suggests that the interaction of the metal d_{xz} orbital with the ligand π_4 is smaller in $Co(\eta^5\text{-}C_9H_7)_2$ and $Co(\eta^5\text{-}C_9Me_7)_2$ than the equivalent interaction in $Co(\eta^5\text{-}C_5H_5)_2$ and $Co(\eta^5\text{-}C_5Me_5)_2$ (d_{xz}–e_{1g}). This may be due to ring slippage. Less destabilization of the metal orbital occurs, and the IE is correspondingly higher. Shifts between the ^3E states of $Co(\eta^5\text{-}C_5H_5)_2$ and the A_1 band of $Co(\eta^5\text{-}C_9H_7)_2$ (0.43 eV) and between $Co(\eta^5\text{-}C_5Me_5)_2$ and the A band of $Co(\eta^5\text{-}C_9Me_7)_2$ (0.5 eV) are in the same direction as the Fe d band; substituting indenyl for cyclopentadienyl *lowers* the IE for these bands. It is difficult, therefore, to categorize the electron-donating or -withdrawing properties of the indenyl and permethylindenyl ligands in the Co systems without specifying the particular MOs under consideration.

The effect on the IE of the a_1 and e_2 band ionizations may be regarded as primarily one of charge and the gross electron-donating and -withdrawing properties of the ligands, whereas that of the e_1 band ionization is a consequence of an orbital effect.

EPR Spectroscopy. The magnetic properties of metallocenes have been thoroughly investigated from both an experimental and theoretical viewpoint.[18,19] The simplest behavior is found for systems with orbitally nondegenerate ground states, i.e. compounds with 15-electron $^4A_{1g}$ ($[Cr(\eta^5\text{-}C_5H_5)_2]^+$) or 20-electron $^3A_{2g}$ ($Ni(\eta^5\text{-}C_5H_5)_2$) configurations. Orbital contributions to the moment are not expected, and the magnetic moments are close to the spin-only value. In contrast, the EPR spectra of ferrocenium cations are only observable in dilute diagmagnetic glasses at liquid-helium temperatures. The d^5 ($(a_{1g})^2(e_{2g})^3$) electronic configuration of the ferrocenium cations results in a $^2E_{2g}$ ground state. This ^2E ground state allows for rapid spin–lattice relaxation and highly anisotropic **g** tensors.[20]

The EPR spectrum of **2** as a frozen glass in CH_2Cl_2 at 4.3 K exhibits an axially symmetrical powder pattern characterized by $g_\parallel = 2.93$ and $g_\perp = 2.15$. Unlike the EPR spectra[21] of the radical cations $[Fe(\eta^5\text{-}C_5H_5)_2]^+$ and $[Fe(\eta^5\text{-}C_5Me_5)_2]^+$, the spectrum was observed up to ca. 100 K indicating that electronic relaxation is not as efficient for **2** as for the unsubstituted metallocenes. The g anisotropy ($\Delta g = g_\parallel - g_\perp$) of 0.78 is significantly lower than 3.08 ± 0.01 found for both the ferrocenium and decamethylferrocenium cations, indicating a different ground-state symmetry for **2** compared to a $^2E_{2g}$ ground state for both $[Fe(\eta^5\text{-}C_5H_5)_2]^+$ and $[Fe(\eta^5\text{-}C_5Me_5)_2]^+$. The assignment of the HOMO in **1** as an A_1 symmetry orbital from photoelectron spectroscopy is entirely consistent with the EPR experiments, which suggest a $^2A_1$ symmetry ground state for the radical-cation **2**.

In addition, the temperature dependence of the integrated signal intensity of the EPR spectrum of a single crystal of **2** obeys the Curie law ($\chi \propto 1/T$) in the temperature range 4–100 K and indicates no long-range magnetic interactions.

In contrast, the variable-temperature EPR spectra for **4** in the temperature range 4.3–298 K on both solid and frozen solutions exhibit characteristic anisotropic patterns with measured g tensors of $g_x = 2.1381$, $g_y = 2.0419$, and $g_z = 1.9429$. The average isotropic g value ($\langle g \rangle$) can be calculated according to $\langle g \rangle^2 = {}^1/_3(g_x^2 + g_y^2 + g_z^2) = 2.0425$.

The temperature dependence of the integrated signal intensity of the EPR spectrum of a single crystal of **4** obeys the Curie law ($\chi \propto 1/T$) in the temperature range 4–100 K and indicates no long-range magnetic interactions.

Magnetic Susceptibility Measurements. The solution magnetic susceptibility of both **2** and **4** have been determined using the Evans method.[22] For a superconducting magnetic field configuration eq 1 is applicable,[13]

$$\chi_M = \left(\frac{3\delta\nu}{4\pi\nu_0 c}\right) + \chi_0 M + \frac{\chi_o(d_o - d_s)}{c} \qquad (1)$$

where $\delta\nu$ = frequency shift (Hz), ν_0 = spectrometer frequency (Hz), χ_M = molar magnetic susceptibility, χ_0 = solvent susceptibility, M = molar weight, d_o = solvent density, d_s = solution density, and c = concentration (mol mL^{-1}).

Since the solution susceptibility and solution density are not known, an accurate measurement of the magnetic moment is best obtained by measuring the variation of the observed shift with temperature. A plot of frequency shift ($\delta\nu$) vs $^1/T$ should be linear with the slope proportional to μ_{eff}. For **2**, a least-squares fit of the frequency shift ($\delta\nu$) vs $^1/T$ gives a room-temperature value of $\mu_{eff} = 2.26 \pm 0.2$ μ_B in CD_2Cl_2 solution.

Using the **g** tensors measured for the EPR spectrum above, we can calculate an effective moment explicitly using eq 2, where $\langle g \rangle^2 = {}^1/_3(g_\parallel^2 + 2g_\perp^2) = 2.41$.

(27) Gassmanan, P. G.; Winter, C. H. *J. Am. Chem. Soc.* **1988**, *110*, 6130.

$$\langle\mu\rangle^2\{[Fe(\eta^5\text{-}C_9Me_7)_2]^+\} = \langle g\rangle^2\{[Fe(\eta^5\text{-}C_9Me_7)_2]^+\}S(S+1) \quad (2)$$

The calculated moment $\mu_{eff} = 2.09$ is equivalent to the measured moment within the experimental error. For **4**, the measured solution magnetic moment $\mu_{eff} = 1.59 \pm 0.2$ μ_B is again in very good agreement with the calculated value of $\mu_{eff} = 1.76$ using the **g** tensors obtained from the EPR spectra.

Solid-State Measurements. Faraday balance magnetic susceptibility measurements in the temperature range 2–300 K indicate that crystals of **2** obeys the Curie Weiss law $\chi^{-1} = C/(T - \Theta)$, with $\Theta = -2.85$ K and an effective moment of 2.09 μ_B. The small negative value of Θ is indicative of weak antiferromagnetic interactions between the radical cations.

Summary

In this paper we have described a convenient synthesis of permethylindene. Treatment of either $FeCl_2$·2THF or $Co(acac)_2$ with the lithium salt of permethylindene (LiInd*) yields the appropriate metal permethylindenyl complexes in good yields. These complexes have low first ionization energies and redox potentials as measured by gas-phase photoelectron spectroscopy and cyclic voltammetry. Both neutral complexes can be oxidized chemically to the monocation. Surprisingly, the Ind* ligand appears to be more electron donating than Cp* for the iron complexes whereas for the cobalt analogue the reverse is found.

Acknowledgment. D.O.H. would like to thank the Science and Engineering Research Council and the Nuffield Foundation for support and S. McLean (CR&D, E. I. du Pont de Nemour) for recording the Faraday magnetic susceptibility experiments. T.M. thanks the Natural Sciences and Engineering Research Council of Canada for support.

Registry No. **1**, 131108-83-3; **2**, 137259-36-0; **3**, 137259-37-1; **4**, 137259-39-3; Li(Ind*), 101960-85-4; tiglic acid, 80-59-1; tigloyl chloride, 35660-94-7; 1,2,3,4-tetramethylbenzene, 488-23-3; 2,3,4,5,6,7-hexamethylindan-1-one, 137175-20-3; heptamethylindene, 86901-30-6.

Theoretical Investigations of Olefin Metathesis Catalysts

Thomas R. Cundari† and Mark S. Gordon*

Department of Chemistry, North Dakota State University, Fargo, North Dakota 58105-5516

Received March 25, 1991

An ab initio analysis of the electronic structure of high-valent, transition-metal alkylidenes as models for olefin metathesis catalysts is presented. The catalyst models studied fall into three categories: "new" metathesis catalyst models—tetrahedral $M(OH)_2(XH)(CH_2)$ complexes; "old" metathesis catalyst models—tetrahedral $MCl_2(Y)(CH_2)$ complexes and alkylidene-substituted Mo metathesis catalysts, $Mo(OH)_2(NH)(=C(H)Z)$. The effect on the bonding caused by modification of either the metal, ligands, or alkylidene substituents is considered. For the new models the minimum energy structures result from maximum metal dπ–ligand pπ bonding and minimum competition among the ligands for the same dπ AO. Rotation about the MC axis increases this competition. The ability of the other multiply bonded ligand (XH) to accommodate the carbene ligand controls the height of the rotation barrier. For Mo and W complexes compression of the M–X–H angle is more facile than that for the Re alkylidene, resulting in a much higher barrier for the latter. A second important result is the greater $M^+{=}C^-$ bond polarity in W versus $Mo(OH)_2(NH)(CH_2)$. Greater polarization correlates with the observed greater metathesis activity for W versus Mo. The bonding in the old models resembles that in the new except for the much greater MC rotational barriers and the lower $M^+{=}C^-$ bond polarity in the former. If greater MC bond polarization does indeed lead to greater reactivity, then one would expect that the old metathesis catalysts are less active compared to their new analogues. Finally, the effects of substitution on the alkylidene ligand of a series of Mo alkylidenes was studied. Electron-withdrawing ligands cause the MC bond length to contract; electron donors have the opposite effect.

I. Introduction

Since the work of Herrison and Chauvin it has been generally accepted that carbene complexes play a pivotal role in transition-metal-catalyzed olefin metathesis, as illustrated in eq 1.[1] The known carbene complexes at that time were the so-called "Fischer-type" carbenes, i.e. a carbene ligand with π-donor substituents attached to a low-valent metal center such as $W(CO)_5(=CMe(OMe))$.[2,3] The carbene C in Fischer-type carbenes is electrophilic and will react with nucleophiles such as phosphines. In 1974 Schrock characterized the first nonheteroatom-stabilized carbene—$(Me_3CCH_2)_3Ta\{=C(H)CMe_3\}$.[4a] This and related compounds, called "Schrock-type" carbenes or alkylidene complexes, were shown to be active in olefin

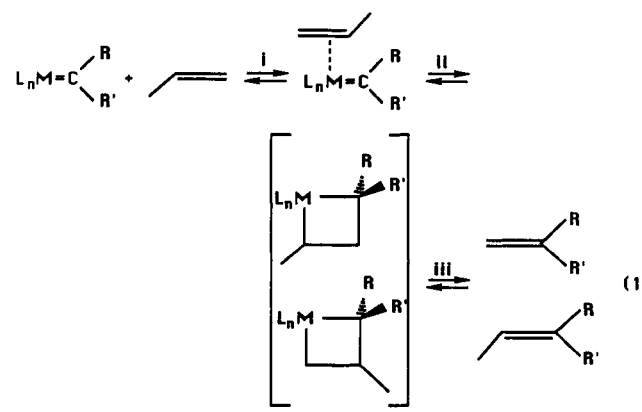

(1)

metathesis and polymerization and for the conversion of carbonyl compounds into olefins (the Wittig synthesis).[4,5]

† Present address: Department of Chemistry, Memphis State University, Memphis, TN 38152.

0276-7333/92/2311-0055$03.00/0